

RSC Advances



This is an *Accepted Manuscript*, which has been through the Royal Society of Chemistry peer review process and has been accepted for publication.

Accepted Manuscripts are published online shortly after acceptance, before technical editing, formatting and proof reading. Using this free service, authors can make their results available to the community, in citable form, before we publish the edited article. This *Accepted Manuscript* will be replaced by the edited, formatted and paginated article as soon as this is available.

You can find more information about *Accepted Manuscripts* in the [Information for Authors](#).

Please note that technical editing may introduce minor changes to the text and/or graphics, which may alter content. The journal's standard [Terms & Conditions](#) and the [Ethical guidelines](#) still apply. In no event shall the Royal Society of Chemistry be held responsible for any errors or omissions in this *Accepted Manuscript* or any consequences arising from the use of any information it contains.

Selective reduction of graphite oxide: A novel approach

Ritwik Panigrahi and Suneel K. Srivastava*

Cite this: DOI: 10.1039/x0xx00000x

Received 00th January 2012,
Accepted 00th January 2012

DOI: 10.1039/x0xx00000x

www.rsc.org/

Graphite oxide (GO) has been selectively reduced (SGO) by H⁺/Na/methanol for conversion of –COOH to –OH groups. An enhanced H-bonding is confirmed between SGO and bistartratocuprate (II)⁴⁻ via FTIR. Graphene/copper nanocomposite subsequently prepared by its in-situ reduction showed superior EMI shielding property compared to conventionally obtained nanocomposites.

The Graphite oxide (GO) also referred as graphitic oxide is an important carbon based layered material.¹ It has been invariably used as a precursor in the synthesis of graphene through variety of processes, such as, mechanical exfoliation, chemical vapour deposition and chemical or thermal reduction for various promising applications.²⁻⁴ The presence of epoxy (-O-), hydroxyl (-OH), carboxylic acid (-COOH) and ketone (C=O) groups on the surface of GO account for its hydrophilic nature and dispersibility in polar medium.^{5,6} These oxygen containing functional groups could also interact and facilitate coordination with metal complexes. In view of this, the present work is focused on preparation of nanocomposites using graphite oxide and Fehling's solution⁷ as sources of graphene and complex of Cu *bistartratocuprate(II)*⁴⁻ respectively. It is anticipated that the presence of -COO⁻ groups in *bistartratocuprate(II)*⁴⁻ complex of Fehling's solution undergoes hydrogen bonding (H-bonding) formation with HO- groups of GO (FSGO).⁸ However, availability of -OH groups undergoing such interaction could be insufficient due to steric crowding created between the -COOH of GO and bulky *bistartratocuprate(II)*⁴⁻ complex of Fehling's solution. As a consequence, the selective transformation of -COOH to -OH group of GO (referred as SGO) appears to be one of the ideal solution to overcome this problem. Therefore, we introduced new approach involving selective reduction of GO through the transformation of -COOH of GO to -COOR group followed by its reduction with Na/CH₃OH to convert it to -OH group according to Bouveault-Blanc⁹ reduction approach. Though, variety of chemical medication of GO are already reported,¹ no such information is available dealing with transformation of -COOH to -OH functionality of GO even till date to our best of our knowledge. Through this approach, more number of -OH groups of SGO compared to GO are likely to interact more with Fehling's solution through H-bonding (FSGO) overcoming thereby the steric

crowding as discussed earlier. When this FSGO is in-situ reduced by hydrazine hydrate, copper nanocomposites of selectively reduced graphite oxide (RSGOCu) are formed. Additionally, it would be interesting to develop, if hydrogen bonded structure between SGO and Fehling's solution could avoid agglomeration of Cu nanoparticles on the RSGO sheet compared to Cu nanocomposites prepared by using directly GO. Detailed preparative method of GO (Hammer's method⁵) followed its selective reduction to prepare RSGOCu nanocomposites (varying proportion of Fehling's solution) is given in supporting information S1 and scheme1. Finally, RSGOCu has been characterized by XRD, FTIR, SEM, TEM, XPS, and conductivity measurements (supporting information S2). EMI shielding property of RSGOCu nanocomposite has also been studied to show the effect of our novel approach during its application.

X-ray diffraction (XRD) showed that the appeared hump at ~24° for 002 planes in SGO and RSGO remains almost unaltered indicating successful reduction of GO by our novel technique. In case of RSGOCu nanocomposites three major peaks at 43.5° (111), 50.5° (200) and 74.5° (220) appeared corresponding to cubic phase of Cu including hump at ~24° for RSGO [JCPDS card No. 4-0836]. (Details in supporting information S3). So our prepared SGO resembles with reported reduced GO with respect to interlayer distance. Figure 1 shows FTIR spectra of RSGOCu₂, RSGOCu₅, RSGOCu₁₀ and Cu nanoparticles. The characteristic bands appeared at 3400, 1720, 1215 and 1580 cm⁻¹ in GO due to stretching vibrations from O-H, C=O, and C-O and skeletal vibrations from unoxidized graphitic domains respectively.

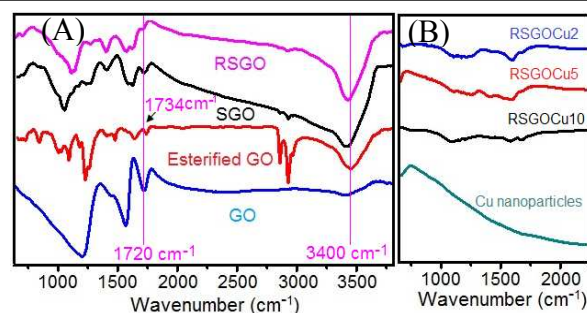
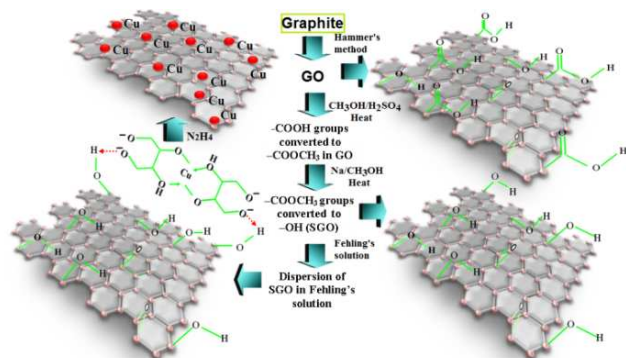


Figure 1 FTIR spectra of (A) GO, esterified GO, SGO, RSGO and (B) RSGOCu



Scheme 1 Schematic representation of selective reduction of GO and formation of RSGOCu nanocomposites

Table 1 Details on sample preparation FSGO1, FSGO2, FSGO3, FSGO4, FSGO5 and FGO* (*prepared by adding 5 ml each of Fehling A and B to dispersed GO in 50 ml of water).

Fehling A (ml)	Fehling B (ml)	H ₂ O (ml)	Amount of SGO (g)	Sample code
1	1	58	0.5	FSGO2
2.5	2.5	55	0.5	FSGO5
5	5	50	0.5	FSGO10
7.5	7.5	45	0.5	FSGO15
10	10	30	0.5	FSGO20

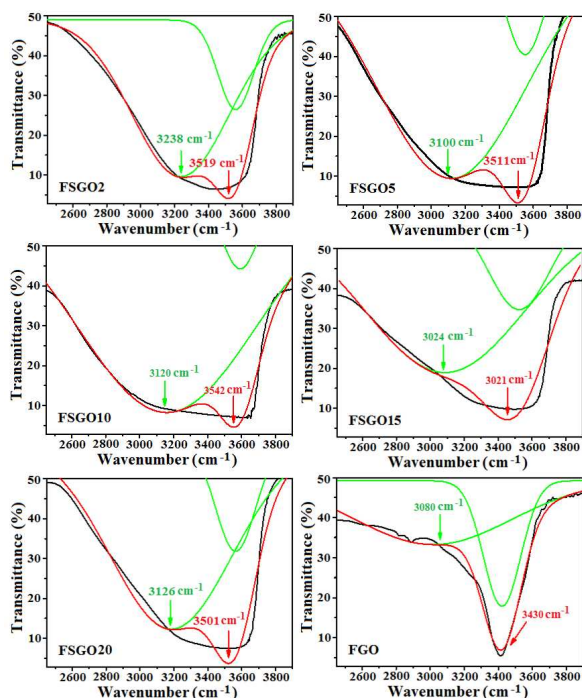


Figure 2 FTIR and deconvoluted FTIR spectra of FSGO2, FSGO5, FSGO10, FSGO15, FSGO20 and FGO10.

These findings confirmed that both $-OH$ and $-COOH$ groups are present in GO.¹⁰⁻¹² After treating GO with CH_3OH/H_2SO_4 , the peak at 1720 cm^{-1} is found to be shifted at 1734 cm^{-1} indicating the transformation of $-COOH$ to $-COOCH_3$ groups. The bands in SGO at 1720 and 1060 cm^{-1} corresponding to $C=O$ and $C-O$ stretching

vibration of $-COOH$ group almost disappeared and respective intensity of 3400 cm^{-1} band due to $O-H$ stretching increased remarkably. These findings clearly demonstrated that $-COOH$ groups in GO are selectively reduced to $-OH$. As expected in case of RSGO, the characteristic peaks at 1720 cm^{-1} ($C=O$) and 1060 cm^{-1} ($C-O$) are diminished, though absorption bands due to skeletal vibrations from unoxidized graphitic domains (1600 cm^{-1}) and $C-OH$ stretching vibrations (1220 cm^{-1}) remained unaltered. When Fehling's solution is added to SGO, it is observed that the peak at 3400 cm^{-1} is blue shifted up to $\sim 3200\text{ cm}^{-1}$ (Table 1, Figure 2 and S4). This evidenced the formation of H bond between $-O-H$ and $-COO^-$ groups of SGO and Fehling's solution respectively (scheme 1). It is also evident from Figure 1 that no remarkable peaks of Cu nanoparticles are present in this region. XPS analysis of samples also supported expulsion of oxygen containing functional group during successive reduction of GO to RSGO and formation of RSGOCu nanocomposites (Supporting information S5). Due to difficulty in differentiation of the overlapping binding energies of carbonyl group of and OH groups, NMR studies on our samples was not carried out.^{13, 14}

SEM and TEM images in Figure 3 (supporting information 6 and 7) further provide visual supports for the formation of RSGOCu nanocomposites. It clearly shows that Cu nanoparticles synthesized from chemical reduction of Fehling's reagent remain in agglomerated state. The high resolution SEM image established that the sizes of the particles to be roughly $\sim 40\text{ nm}$. SEM of RSGO shows the formation of sheet like structure quite similar to reduced graphite oxide reported earlier.¹⁵ It is also evident from Figure 3 that Cu nanoparticles are well dispersed on the RSGO sheet in RSGOCu nanocomposite, which is also supported by TEM analysis. TEM images of RSGOCu10 and RGOc10 are further confirmed the particle size of Cu nanoparticles to be $\sim 40\text{ nm}$ similar to as observed through SEM images. In case of RSGO, the formation of sheet like reduced graphite oxide sheets are clearly visible. TEM image also shows that RSGO sheets acquired several hundred square nanometers area and are rippled/entangled with each other. A fraction of RSGO sheets (marked with arrow) also appeared as transparent mono layer.¹⁶ In addition, during TEM analysis it is observed that hydrazine hydrate reduced SGO, i.e. RSGO, is quite stable under the

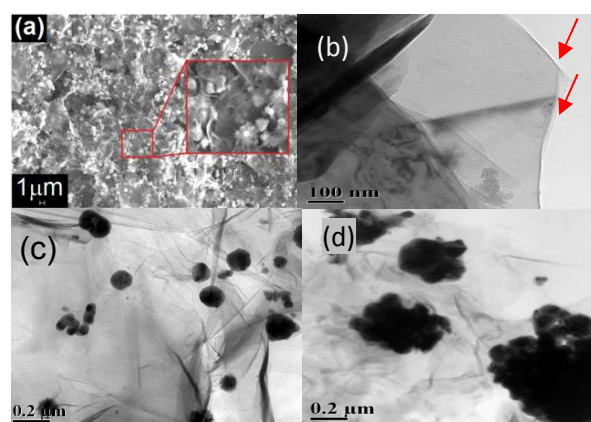


Figure 3 (a) SEM images RSGOCu10, TEM images of (b) RSGO, (c) RSGOCu10, and (d) RGOc10.

electron beam. Figure S7 (supporting information S7) also shows the formation of scrolled RSGO nanosheets probably due to its intrinsic property of microscopic crumpling through bending and buckling accounting for the thermodynamic stability of 2D membrane. In addition the presence of disordered graphite lattice is probably due to the partial restoration of graphite lattice from disorder to order

crystal structures. TEM image of RSGOCu10 is indicating that the Cu nanoparticles are well dispersed and acts as to interconnect between successive RSGO wrapped sheets. This is in contrast to RSGOCu10 nanocomposites obtained by in-situ reduction of GO and Fehling's solution, where agglomeration of Cu is clearly evident from the corresponding TEM image. SEM and TEM studies supported the findings of FTIR and TGA (supporting information S8) that graphene/Cu composites takes place through the combination of SGO and Fehling's reagent followed by in-situ reduction.

Figure 4 displays the corresponding Raman spectra of GO, SGO, RSGO, RSGOCu2, RSGOCu5 and RSGOCu10. Two distinct peaks appeared in the spectra of GO at 1351 (D band) and 1578 cm^{-1} (G band).¹⁷ The G band corresponds to the in-plane vibration of the sp^2 atoms of hexagonal graphite lattice is a doubly degenerate phonon mode (E_{2g} symmetry) at the Brillouin zone center.^{18,19} D band appears due to the breathing mode of κ - point phonons with A_{1g} symmetry.²⁰ In addition, GO exhibits intensity ratio (I_D/I_G) of D to G band i.e. 0.94 due to defects and disorders originating from carboxylic and other functionality present on its surface.²¹ When GO is selectively reduced to transform -COOH to -OH functionality, higher value of I_D/I_G (1.05) of SGO could account for the formation of new graphitic domain. After reduction of SGO to RSGO, it is observed that its G band (1578 cm^{-1}) is down-shifted to 1573 cm^{-1} . This is due to the selective reduction of isolated double bonds in C=O, -COOH followed by hydrazine hydrate reduction.²² In case of RSGO, the I_D/I_G value is found to be 1.12 which is probably due to the formation of better graphitic domain compared to SGO. When SGO and Fehling's solution together are in-situ reduced by N_2H_4 , no additional peaks of copper are observed in Raman spectra of produced RSGOCu nanocomposites in the selected range. However, intensity of both D and G bands are found to be reduced considerably in Cu loaded RSGO samples. It may be attributed due to the presence of conducting Cu nanoparticles which shield the incident laser beam to interact with layers of RSGO. However, it is clear that considerable structural as well as chemical changes occur during the successive transformations of GO to SGO followed by RSGO, RSGOCu2 and RSGOCu5 and RSGOCu10. Room temperature D.C. electrical conductivity (σ_{RT}) measurements have

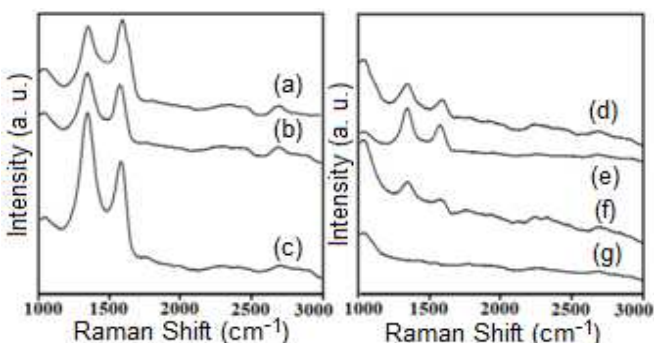


Figure 4 Raman spectra of (a) GO, (b) SGO, (c) RSGO, (d) RSGOCu2, (e) RSGOCu5, (f) RSGOCu10 and (g) Cu nanoparticles.

also been carried out on RSGO and corresponding Cu loaded samples (Figure 5 and Supporting information S9). It is inferred the σ_{RT} values of RSGO, RSGOCu2, RSGOCu5 and RSGOCu10 are found to be 4.58, 29.919, 523.3 and 3896.5 Sm^{-1} respectively. This clearly indicates that conductivity increases with Cu loadings and attains nearly 850 times more in RSGOCu10 with respect to RSGO alone. Interestingly, such high value of conductivity in metal/graphene nanocomposites has never been reported earlier in the literatures. We have also prepared copper nanocomposite of

graphene (RSGOCu10) by in situ reduction of GO and Fehling's solution maintaining other conditions similar to preparation of RSGOCu10 earlier. As expected, we found that room temperature electrical conductivity of RSGOCu10 (600.5 Sm^{-1}) was significantly low compared to RSGOCu10 (3896.5 Sm^{-1}). All these findings clearly demonstrate that a continuous electronic path has been formed by deposition of highly conducting Cu nanoparticles on RSGO sheets which could account for observed enhancement in electrical conductivity. The presence of free electrons in mono dispersed metallic Cu nanoparticles (σ_{RT} 1.59x10⁷ Sm^{-1}) could account for the formation of more conducting electronic pathways in RSGOCu nanocomposites. On the other hand RSGOCu nanocomposite could unable to achieve this for agglomeration of Cu nanoparticles. As a result, the successive increment in its D.C. conductivity is observed with increasing Cu loading in RSGO, a fact also reflected from EMI SE measurements as discussed below.

Fig. S10 (Supporting Information S10) represent variation of reflection loss versus frequency (2-8 GHz) for RSGO, RSGOCu10, RSGOCu1, RSGOCu5 and RSGOCu10. The corresponding values are found to be in the range of -4.34 to -6.5, -8 to -4.8 and -4.5 to -2.6, -0.34 to -0.83 and -1.14 to -0.5 dB. These findings clearly suggest that Cu loaded RSGO exhibit higher reflection loss with respect to RSGO. This could be attributed to the increase in D.C. conductivity of Cu loaded RSGO nanocomposites.²³ Figure 6 displays variation of EMI shielding effectiveness of RSGO and its copper loaded nanocomposites in the frequency range 2-8 GHz. These findings show that EMI shielding effectiveness of RSGOCu nanocomposites is dependent on Cu loadings and frequency. It is noted that EMI shielding effectiveness of all the Cu filled RSGO nanocomposites is always higher than the neat RSGO over the entire frequency range.

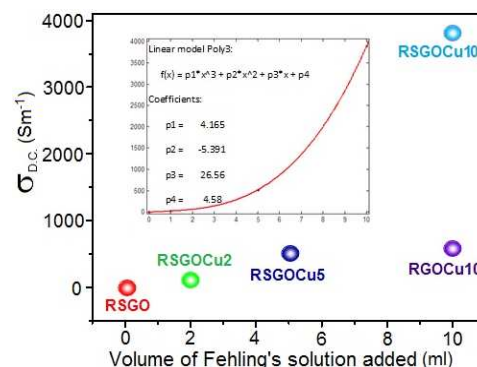


Figure 5 Variation of room temperature D.C. conductivity ($\sigma_{\text{D.C.}}$) of RSGO and its Cu nanocomposites with volume of Fehling's solution. (Inset: polynomial fitting curve)

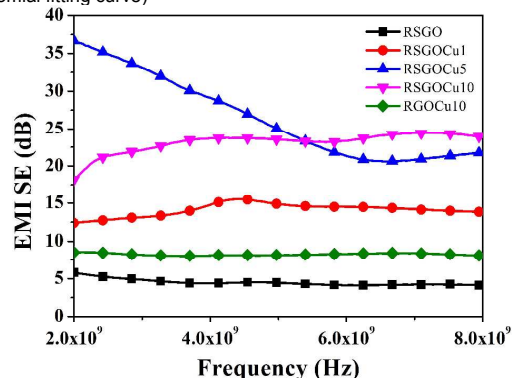


Figure 6 Variation of EMI shielding versus frequency (2-8 GHz) of RSGO, RSGOCu10, RSGOCu2, RSGOCu5 and RSGOCu10

Further, it is also observed that EMI shielding effectiveness of RSGO, RGO/Cu10, RSGO/Cu2, RSGO/Cu5, RSGO/Cu10 are found to be 4, 8, 14, 20, 24 dB at ~7 GHz and 6.8, 5.12, 35, 20 dB at ~2-6 GHz respectively. This clearly suggests that reflection accounts for the major contribution in total EMI shielding. These findings also strengthen earlier suggestions that conductivity could play an important role in influencing total EMI shielding of the composites.

It may be noted that the target value of EMI shielding effectiveness needed for commercial application is ~ 20 dB (equal to or less than 1% transmittance of electromagnetic wave). Therefore, it is anticipated that developed RSGO/Cu5 and RSGO/Cu10 could find better commercial applications. The complex permittivity ($\epsilon^* = \epsilon' - i\epsilon''$) has been calculated using the scattering parameters (supporting information S10) S_{11} and S_{21} obtained from VNA instrument followed by applying standard Nicholson-Ross and Weir theoretical calculations.²⁴ Figure S10 (Supporting information S10) shows variation of room temperature frequency dependence of relative complex permittivity (ϵ^*) of pure RSGO and RSGO/Cu composites. It may be mentioned that the real part of ϵ^* (ϵ') is related to polarization of the materials. When polarization is increased, the storage capacity of the electrical energy is also enhanced.²⁵ Actually conductivity of Cu is higher compared to RSGO which increases the conductivity of the corresponding composites resulting in the increments of the values of ϵ' and ϵ'' . Our observation is quite relevant with the previous reports where loading of Ag nanoparticles was responsible for the increments of the values of ϵ' and ϵ'' in polyaniline/graphene/Ag composites.²⁶ It is well-known that dipolar and electrical polarization in a material are induced in presence of microwave by its polarizability, which is influenced by the permittivity which depends on conductivity and electric polarization of a material. So for that reason it can be said that with increasing conductivity the values of ϵ' and ϵ'' increases. Interestingly it is observed that in case of RGO/Cu10 the values of ϵ' and ϵ'' are in the range 25 - 14 and 7 - 4.5 respectively. It is anticipated that free electron of copper and π electron clouds of graphene together induces the enhanced polarization under microwave irradiation. As a result, the electronic flux increases in the composites with Cu loading, a fact already established in permittivity discussion. All these findings also support the highest values of ϵ' , ϵ'' and $\tan\delta_E$ achieved in RSGO/Cu10. In all probability, the increased random collision between the free electrons at such higher loading of Cu in RSGO is likely to be hindered leading to the dissipation of electromagnetic energy as heat. Also it leads dielectric loss in presence of a continuous conducting network due to accumulation of charges on the interfacial region to form large dipoles. SEM and TEM also established earlier that in RGO/Cu10 perfect conducting network has not been formed and is reflected in the values of $\tan\delta_E$. We also noticed that RGO/Cu10 shows large decrease in ϵ' , ϵ'' and $\tan\delta_E$ compared to RSGO/Cu10 due to its relatively low conductivity. In addition, lower values of ϵ' and ϵ'' due to the interfacial polarization between RGO/Cu and RSGO/Cu also cannot be ruled out.

In summary graphite oxide (GO) has been selectively reduced by Bouveault-Blanc approach to selectively reduced graphite oxide (SGO). Subsequently, SGO and Fehling's reagent has been in-situ reduced by N_2H_4 to prepare RSGO/Cu nanocomposites. The formation and morphology of the products at different stages has been supported by XRD, FT-IR, SEM, TEM and Raman analysis. FT-IR of RSGO showed enhanced interaction between -OH (SGO) and -COO⁻ (Fehling's reagent) leading to the better dispersion of Cu

nanoparticles on RSGO sheets during its in-situ reduction. Room temperature D. C. conductivity improvement was found to be ~850 times in RSGO/Cu10 compared RSGO. In addition, improvement in conductivity was found to be 70-80 times in RGO/Cu10 in absence of Bouveault-Blanc approach. In EMI shielding application (2-8 GHz) RSGO/Cu10 showed 6-8 times more efficiency compared to RGO/Cu10. Our findings clearly demonstrated that the selective reduction of GO monitored the dispersion of Cu nanoparticles on graphene (RSGO) sheet accounts for such significant enhancement in conductivity, which in turn are reflected in their EMI shielding performance. To our belief, such novel technique involving selective reduction of GO could open a new scope in future.

The authors are grateful to UGC and CSIR New Delhi, India for providing financial supports and facilities.

Notes and references

- (1) (a) A. H. Castro Neto, F. Guinea, N. M. R. Peres, K. S. Novoselov, A. K. Geim, *Rev. Mod. Phys.* 2009, **81**, 109. (b) S. K. Srivastava, J. J. Pionteck, *Nanosci. Nanotech.* 2014, **15** (In press).
- (2) F. Banhart, J. Kotakoski, A. V. Krasheninnikov, *ACS Nano*, 2010, **5**, 26.
- (3) K. Hu, D. D. Kulkarni, I. Choi, V. V. Tsukruk, *Prog. Polym. Sci.* 2014, DOI: 10.1016/j.progpolymsci.2014.03.001.
- (4) F. Xia, D. B. Farmer, Y. M. Lin, P. Avouris, *Nano Lett.* 2010, **10**, 715.
- (5) W. S. Hummers, R. E. Offeman, *J. Am. Chem. Soc.* 1958, **80**, 1339.
- (6) A. Dimiev, D. V. Kosynkin, L. B. Alemany, P. Chaguine, J. M. Tour, *J. Am. Chem. Soc.* 2012, **134**, 2815.
- (7) H. Fehling, *Ann. Chemie und Pharmacie.* 1849, **72**, 106.
- (8) (a) H. K. Jeong, H. J. Noh, J. Y. Kim, M. H. Jin, C. Y. Park, Y. H. Lee, *EPL*, 2008, **82**, 67004. (b) K. A. Mkhoyan, A. W. Contryman, J. Silcox, D. A. Stewart, G. Eda, C. Mattevi, S. Miller, M. Chhowalla, *Nano Lett.* 2009, **9**, 1058-1063. (c) T. Szabo, O. Berkesi, P. Forgo, K. Josepovits, Y. Sanakis, D. Petridis, I. Dekany, *Chem. Mater.* 2006, **18**, 2740-2749.
- (9) (a) L. Bouveault, G. Blanc, *Compt. Rend.* 1903, **136**, 1676. (b) L. Bouveault, G. Blanc, *Bull. Soc. Chim. France*, 1904, **31**, 666.
- (10) M. Mermoux, Y. Chabre, A. Rousseau, *Carbon*, 1991, **29**, 469-474.
- (11) T. Szabo, O. Berkesi, P. Forgo, K. Josepovits, Y. Sanakis, D. Petridis, I. Dekany, *Chem. Mater.* 2006, **18**, 2740-2749.
- (12) T. Szabo, E. Tombacz, E. Illes, I. Dekany, *Carbon*, 2006, **44**, 537-545.
- (13) D. W. Lee, V. Santos, L. De Los, J. W. Seo, L. L. Felix, A. D. Bustamante, J. M. Cole, C. H. W. Barnes, *J. Phys. Chem. B*, 2010, **114**, 5723-5728.
- (14) M. Acik, G. Lee, C. Mattevi, A. Pirkle, R. M. Wallace, M. Chhowalla, K. Cho, and Y. Chabal, *J. Phys. Chem. C*, 2011, **115**, 19761-19781
- (15) A. P. Singh, M. Mishra, P. Sambyal, B. K. Gupta, B. P. Singh, A. Chandra, S. K. Dhawan, *J. Mater. Chem. A*, 2014, **2**, 3581
- (16) D. D. L. Chung, *Carbon*, 2001, **39**, 279-285.
- (17) J. Gao, F. Liu, N. Ma, Z. Wang, X. Zhang, *Chem. Mater.* 2010, **22**, 2213.
- (18) M. A. Pimenta, G. Dresselhaus, M. S. Dresselhaus, L. G. Cancado, A. Jorio, R. Saito, *Phys. Chem. Chem. Phys.* 2007, **9**, 1276.
- (19) J. Tian, S. Liu, Y. Zhang, H. Li, L. Wang, Y. Luo, A. M. Asiri, A. O. A. Youbi, X. Sun, *Inorg. Chem.* 2012, **51**, 4742-4746
- (20) D. Graf, F. Molitor, K. Ensslin, C. Stampfer, A. Jungen, C. Hierold, L. Wirtz, *Nano Lett.*, 2007, **7**, 238.
- (21) W. F. Chen, L. F. Yan, P. R. Bangal, *J. Phys. Chem. C*, 2010, **114**, 19885.
- (22) C. Xu, X. Wang, J. W. Zhu, *J. Phys. Chem. C*, 2008, **112**, 19841.
- (23) G. A. Gelves, M. H. Al-Saleh, U. J. Sundararaj, *Mater. Chem.* 2011, **21**, 829-836.
- (24) A. M. Nicolson, G. F. Ross, *IEEE Trans. Instrum. Meas.*, 1968, **IM-17**, 395
- (25) C. Wang, X. J. Han, P. Xu, X. L. Zhang, Y. C. Du, S. R. Hu, *Appl. Phys. Lett.* 2011, **98** (7), 072906-9
- (26) Y. Chen, Y. Li, M. Yip, N. Tai, *Composite Sci. Technol.* 2013, **80**, 80